物理学論文選集 I

有機超伝導体の物性

石黒武彦　責任編集

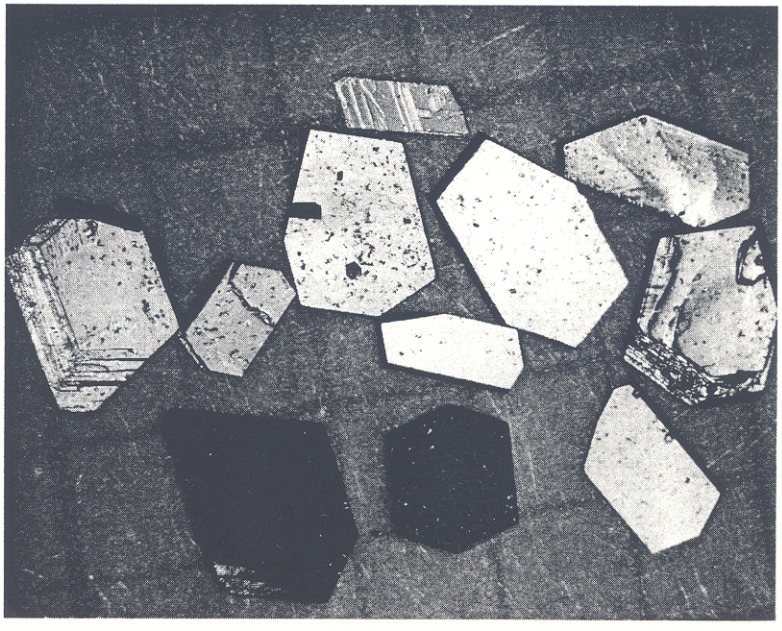

社団法人　日本物理学会

Acknowledgment

The Physical Society of Japan has the pleasure of presenting this issue of the "Selected Papers in Physics". The present volume contains papers in the field of

Organic Superconductors
(edited by Takehiko Ishiguro)

appearing in different journals in USA, Europe and Japan.

The publication of this volume, which was planned to comply with eager wishes of the members of the Physical Society of Japan, has been made possible through the kind cooperation of both the authors and the publishers of respective journals who granted permission for reproduction.

We express our sincere gratitute and deep appreciation to the following publishers and the authors including those of Article III for their kind cooperation.

Publisher	Journal	Article
The American Physical Society	Phys. Rev.	I,IV,XI,XIV
American Institute of Physics	JETP Lett.	V
Société Française de Physique	J. Phys. Lett., Paris	II
	J. Phys., Paris	IX,XII
American Chemical Society	Inorg. Chem.	VIII
	J. Am. Chem. Soc.	XV
Pergamon Press PLC	Solid State Commun.	X
The Chemical Society of Japan	Chem. Lett.	VII
	Bull. Chem. Soc. Jpn.	XIII
Publ. Office Japan. J. Appl. Phys.	Jpn. J. Appl. Phys.	VI

Also some figures in the review article in Japanese were reproduced from several journals, owing to the kind permission granted by authors and publishers. We thank authors and journals listed below.

Author(s)	Journal	Figure in the Japanese article
A. F. Garito et al.	J. Am. Chem. Soc.	Fig. 1
K. Bechgaard	Mol. Cryst. Liq. Cryst.	Fig. 5(a) (b)
I. F. Schegolev	Jpn. J. Appl. Phys. Suppl.	Fig. 9
D. Jérome et al.	Phys. Rev. Lett.	Fig. 13
K. Kajita et al.	Solid State Commun.	Fig. 14
C. S. Jacobsen et al.	Phys. Rev. Lett.	Fig. 15

Michiji Konuma
President
The Physical Society of Japan

Each volume in the "Series of Selected Papers in Physics" is printed by the Physical Society of Japan for use by its members only.

物理学論文選集 I　　有機超伝導体の物性

編集兼発行者	社団法人 日本物理学会
	105 東京都港区芝公園3丁目5番8号 機械振興会館211号室
印刷者	小宮山一雄
印刷所	小宮山印刷工業㈱
	162 東京都新宿区天神町78

1992年3月20日 印刷・発行

ISSN 0549-5016

Reprinted from J. Phys., Paris 44 C3 (1983) 847-857
by permission of the Société Française de Physique and the authors

JOURNAL DE PHYSIQUE

Colloque C3, supplément au n°6, Tome 44, juin 1983 page C3-847

ELECTRONIC STRUCTURE OF THE 2:1 CHARGE TRANSFER SALTS OF TMTCF

P.M. Grant

IBM Research Laboratory, 5600 Cottle Road, San Jose, California 95193, U.S.A.

Résumé — Nous présentons un modèle unifié à une particule capable d'expliquer plusieurs faits expérimentaux obtenus sous hautes et basses températures et/ou pressions. Une attention spéciale a été portée sur la nature et l'origine des interactions entre chaînes permettant d'expliquer un grand nombre des propriétés physiques de ces matériaux.

Abstract — We present a unified single-particle model capable of explaining a number of experimental facts pertaining to the high and low temperature/pressure regimes of $(TMTCF)_2X$. Special attention is paid to the nature and source of the interchain interaction in determining the overall physical properties of these materials.

1. Introduction.— Tetramethyltetrachalcogenafulvalene, TMTCF (C = S, Se, Te), forms a number of simple 2:1 salts with a wide variety of monovalent inorganic ions. These materials exhibit a rich spectrum of physical phenomena as a function of temperature and pressure. Among the outstanding features are their high room temperature conductivity, the occurrence of a metal-insulator transition due to spin density wave condensation (antiferromagnetism) or anion ordering, and, in certain of the selenium compounds, the onset of superconductivity at low temperature and moderate pressure[1].

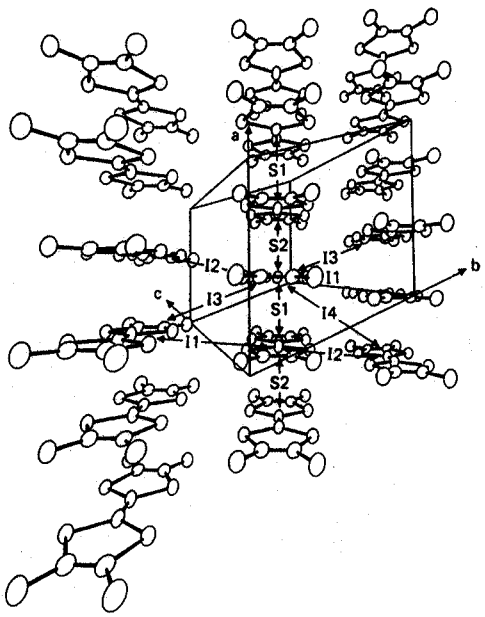

Fig. 1. Perspective view of the $(TMTCF)_2X$ crystal structure.

In this paper we present a unifying framework for the electronic properties of $(TMTCF)_2X$ based on simple one-electron concepts. We divide the problem into two separate but related areas: a high temperature regime characterized by an open, quasi-planar Fermi contour, and a low temperature regime dominated by spin and/or anion order symmetry breaking of the high temperature band structure. In both cases we will show that interchain interactions play a significant role.

Figure 1 depicts the general features of the $(TMTCF)_2X$ cation lattice. The view is down the long axis of the central cation as seen in perspective with respect to the perpendicular bisector plane through the midpoint of the C=C interfulvalene bond of the central cation. We show a single sheet of stacks generated by translation along the b-direction. The cation sheets are separated by anion planes with each anion located at a corner of the indicated unit cell. Figure 1 also contains the six most probable interaction directions for electronic overlap in $(TMTCF)_2X$.

Two are in the stacking, or a, direction and four are in the interstack, or b, direction. For the interstack directions shown, we designate I1 as the interaction between the closest neighbor, I2 as that in the negative b-direction and slightly more removed, and I3, generated by a pure b-axis translation, as that for the third nearest neighbor. The fourth nearest neighbor interaction, I4, is between the central cation and its neighbor in the (−1, 1) direction. The I1 and I2 interactions form a sheet of alternating cations in the b-direction and would seemingly comprise the plane of strongest interchain coupling. Each inter-selenium distance is approximately equal to a van der Waals radius of 3.8Å, being slightly smaller for I1, slightly larger for I2, and about 10 percent larger for I3. I4 is about 20 percent greater than van der Waals. Note that the closest, I1, has essentially one Se-Se contact with the central cation while I2 has two. Figure 1 shows the $(TMTCF)_2X$ stack to be slightly dimerized with two cations per unit cell. This small amount of dimerization may seem surprising in a conducting charge transfer salt due to the concomitant gap introduced in the electronic structure; however, because of the 2:1 stoichiometry, this gap is not at the Fermi energy. In analogy to the interchain case, we refer to the two possible intermolecular interactions as S1 and S2, ordered with respect to increasing separation. Note that we have not considered any interactions in the c-axis direction. Direct calculation indicates these are small compared to the b-axis interaction[2]. For our purposes here, we will consider only the two-dimensional aspects of the $(TMTCF)_2X$ band structure. Also, we neglect any effect of the anions on the energy band dispersion which we take to arise solely from the various cation interactions just described. The anions play a central perturbative role in determining cell symmetry and in band gap production.

2. Model dispersion equation.— The complete crystal secular equation arising from a Bloch-adapted non-orthogonal LCAO basis set is

$$\sum_{\rho j} \left\{ \sum_{\ell} e^{i\vec{k}\cdot\vec{R}_\ell} [H_\ell(\rho' j', \rho j) - E S_\ell(\rho' j', \rho j)] \right\} C_{\rho j} = 0 , \tag{1}$$

where the matrix element of a general operator $\mathcal{O}$ ($\mathcal{O}$ = H or S, the unit operator) is given by

$$\mathcal{O}_\ell(\rho' j', \rho j) = \int d^3r \; \varphi^*_{\rho'}(\vec{r} + \vec{R}_\ell - \tau_{j'}) \, \mathcal{O} \, \varphi_\rho(\vec{r} - \tau_j) . \tag{2}$$

The vectors $\vec{k}$ and $\vec{R}_\ell$ have their usual meaning as crystal momentum and unit cell translation, respectively, with ℓ an integer triad designating a particular translation direction. The non-vanishing off-diagonal elements of S, the overlap matrix, follow from the non-orthogonality of the LCAO basis set $\{\varphi_\rho(\vec{r} - \tau_j)\}$ where ρ indexes a given atomic orbital and τ_j is the vector position of that orbital in the direct lattice unit cell. Thus, considering only the cation components of $(TMTCF)_2X$, τ_j would span four seleniums, ten carbons and 12 hydrogens, twice, for a total of 52 atomic positions. Taking Se 4s, Se 4p, C 2s, C 2p and H 1s as the relevant bonding orbitals then yields a basis set of 136 elements, or, 76 occupied bands when all electrons are accounted for. It is, of course, possible to attack Eq. (1) directly and solve for all 76 bands, but clearly, some simplifications are necessary if one is to gain any useful insights into the overall electronic structure of these systems. We therefore make the following assumptions: (1) we replace the methyl groups by hydrogen, *i.e.*, we make TMTCF into TCF; (2) we assume that we have already solved for the isolated molecular orbital states and now employ these as the new basis set $\{\varphi_\rho(\vec{r} - \tau_j)\}$, and, finally; (3) that we use the highest occupied molecular orbital (HOMO) as the only state which will be relevant to transport in the solid. Immediately we have reduced the number of bands to be considered to two. We justify our individual assumptions on the following grounds: (1) that the intermolecular overlaps are dominated by the chalcogenide atomic orbitals; (2) the intermolecular interactions are weak compared to intramolecular, and; (3) the isolated cation molecular orbitals are well separated from each other with respect to the conduction band width. Equation (1) then reduces to a simple tight-binding dispersion relation involving six transfer integrals representing the six interactions of Fig. 1:

$$E(\vec{k}) = 2[t_{I3} \cos \vec{k}\cdot\vec{b} + t_{I4} \cos \vec{k}\cdot(\vec{a} - \vec{b})] \pm |T(\vec{k})| , \tag{3a}$$

$$T(\vec{k}) = t_{S2} + t_{S1} e^{-i\vec{k}\cdot\vec{a}} + t_{I2} e^{-i\vec{k}\cdot\vec{b}} + t_{I1} e^{-i\vec{k}\cdot(\vec{a}-\vec{b})} . \tag{3b}$$

Since the intermolecular overlaps are $\leq 10^{-2}$, we have omitted them in deriving Eqs. (3). Equations (3) provide a complete analytical description of the 2D band structure of $(TMTCF)_2X$ which can be used as the basis for the derivation of further electronic and transport properties. The vectors a and b are the unit cell parameters of Fig. 1 represented in a cartesian coordinate system. Anticipating that we will be dealing with a quarter-empty conduction band and that the numerical calculations will show $t_{I1} << t_{I2} \approx t_{I3}$ and $t_{S1} \approx t_{S2}$, further simplification is possible. Near E_F, we may set $t_{I4} = t_{I1} = 0$, and define the effective transfer integrals $t_I = t_{I3} + t_{I2}/2$ and $t_S = (t_{S1} + t_{S2})/2$. Eqs. (3) then yield for the total dispersion

$$E(\vec{k}) = 2(t_I \cos \vec{k}\cdot\vec{b} \pm t_S \cos \frac{1}{2} \vec{k}\cdot\vec{a}) \, . \tag{4}$$

This equation represents the greatest possible simplification. At the expense of sacrificing all zone boundary splittings it will nevertheless replicate quite well the 2D band structure near the Fermi energy, E_F.

3. Transfer integral calculation.— Each of the transfer integrals in Eqs. 3 was taken to be half the magnitude of the splitting of the monomer HOMO level for a dimer cation pair formed in the appropriate interaction direction. The phase of a particular transfer integral was determined from the sign of the associated dimer overlap integral. The dimer splitting was calculated in the Mulliken-Wolfsberg-Helmholtz (MWH)[3] approximation in which the Hamiltonian matrix elements of Eqs. (1) and (2) are assumed proportional to the overlap integral as follows:

$$H_I(\rho'j',\rho j) = K \, S_I(\rho'j',\rho j) \, (E_{\rho'j'} + E_{\rho j})/2 \, , \tag{5}$$

where $E_{\rho'j'}$, $E_{\rho j}$ are the one-electron "ionization potentials" and $S_I(\rho'j',\rho j)$ the overlap matrix computed directly from the basis set via Eq. (2). K is an empirical scaling parameter which we took equal to 1.75 in common with other workers using this method. It is also common practice to choose atomic Slater-type-orbitals (STO's) as the analytic form of the basis set used to calculate $S_I(\rho'j',\rho j)$ and to take either calculated or experimental values for the one-electron ionization potentials $E_{\rho j}$ in the construction of $H_I(\rho'j',\rho j)$ via Eq. (5). The total STO wavefunction is given by

$$\varphi_{\rho_{nlm}}(\vec{r}) = R_{nl}(r) \, Y_{lm}(\theta,\phi) \, , \tag{6}$$

where

$$R_{nl}(r) = \sum_{\lambda(l)} C_{n_\lambda} \, [(2n_\lambda)!]^{-1/2} \, (2\zeta_\lambda)^{n_\lambda+1/2} \, r^{n_\lambda-1} \, e^{\zeta_\lambda r} \, . \tag{7}$$

Here $Y_{lm}(\theta,\phi)$ is the usual normalized spherical harmonic. Equation (7) expresses the radial part of φ as a linear combination of normalized STO's where the coefficients C_{n_λ} and exponents ζ_λ are variationally computed by self-consistent-field (SCF) techniques to minimize the total atomic electronic energy. Tables of C_{n_λ} and ζ_λ for the elements can be found in several standard reference works[4]. In an earlier paper[5], we had used a basis set consisting of only one STO (single-ζ) for each valence orbital on each atom in the TMTCF molecule. The use of single-ζ basis sets is a common practice among users of the MWH method for reasons of obvious computational efficiency. However, for $(TMTCF)_2X$, the intermolecular distances over which the electronic interactions of interest occur are large, and although the magnitude of the wavefunction and associated overlap integral are small, the long range details of the basis set are crucial. That is, the SCF procedures used to compute C_{n_λ} and ζ_λ tend to concentrate charge density at normal orbital radii. Thus, if only one STO is used to approximate a given valence orbital, the effect of the SCF optimization results in a ζ that puts as much charge as possible on the shell radius and which does not represent properly the true diffuse character of the orbital wavefunction. This shortcoming is resolved by employing Eq. (7) in its multi-ζ form. Therefore, one might expect multi-STO's to provide a much better representation for the calculation of intermolecular overlaps in organic molecular crystals. In fact, the multi-ζ STO's for Se 4s and Se 4p approximate numerical Hartree-Fock results to within a few percent for distances out to 5 Å from the nuclear center.

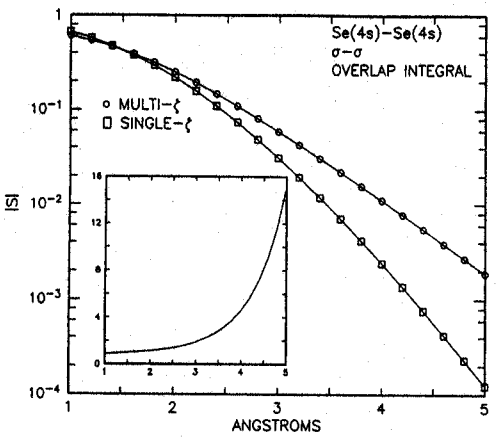

Fig. 2. Comparison of Se 4s σ-overlap integrals for single-ζ and multi-ζ STO basis sets. Inset gives percent difference with distance.

The results of choosing multi-ζ *vs.* single-ζ STO's on the interatomic selenium 4s - 4s σ overlap are shown in Fig. 2. Little difference is observed in the 1-2 Å region of usual intramolecular bonding, but beyond 3 Å, the region of intermolecular separation, the single-ζ magnitudes fall 3-16 times below those values obtained from a multi-ζ basis set, with concomitant effects on the associated transfer integrals. Similar results are obtained for other chalcogenide and carbon σ and π overlaps. All previous MWH calculations on charge transfer salts used single-ζ wave functions. It now appears that band dispersions obtained therefrom are far too small, both in the stacking and interchain directions. If one proceeds on the assumption that the optimal basis set to use in MWH calculations is the one which most closely approximates one-electron atomic Hartree-Fock values, then it is critical that multi-ζ STO's be employed[6].

The resulting transfer integral values for $(TMTSF)_2X$ and $(TMTTF)_2X$ are shown in Tables I and II below[7].

Table I. Transfer integrals and band structure parameters for $(TMTSF)_2X$ compounds of known crystal structure. All energies are in meV ($\times 10^{-3}$ eV).

X	t_{S1}	t_{S2}	t_{I1}	t_{I2}	t_{I3}	t_{I4}	t_S	t_I	t_S/t_I	$t_{S1}-t_{S2}$	E_F
ReO_4	390	338	−15.0	−54.5	43.2	11.8	364	19.7	18	52	255
ClO_4	393	339	−15.3	−54.4	45.1	11.5	366	21.6	17	54	260
FSO_3	386	339	−14.9	−53.8	45.4	11.8	363	22.1	16	47	260
NO_3	407	374	−14.2	−51.3	46.5	12.4	391	23.9	16	33	285
PF_6 (4K)	422	337	−18.0	−45.2	45.0	14.3	380	23.9	16	85	279
H_2F_3	425	374	−13.9	−45.0	41.5	11.0	400	21.4	19	51	283
PF_6 (300K)	395	334	−9.5	−36.2	41.5	9.9	365	26.2	14	61	273
AsF_6	397	340	−7.6	−29.9	38.9	9.5	369	26.3	14	57	279
Mean	402	347	−13.6	−46.3	43.3	11.5	374	23.1	16	55	272
%RMS	3.7	4.9	25	20	5.9	13	3.7	10.1	11	27	12

Table II. Transfer integrals and band structure parameters for $(TMTTF)_2X$ compounds of known crystal structure. All energies are in meV ($\times 10^{-3}$ eV).

X	t_{S1}	t_{S2}	t_{I1}	t_{I2}	t_{I3}	t_{I4}	t_S	t_I	t_S/t_I	$t_{S1}-t_{S2}$	E_F
Br	256	223	−12.8	−36.7	26.9	8.8	240	10.0	24	33	163
BF_4	261	194	−8.0	−28.5	24.4	7.3	228	12.7	18	67	159
SCN	214	211	−4.8	−18.9	17.1	6.7	213	8.8	24	3	151
ReO_4	214	185	−1.2	−18.5	17.9	5.8	200	11.4	17	29	147
Mean	236	203	−6.7	−25.7	21.6	7.2	220	10.7	21	33	155
%RMS	11	8	74	34	22	18	7.9	15.9	18	80	7.3

The average anisotropy t_S/t_I is approximately 16 for $(TMTSF)_2X$ and 21 for $(TMTTF)_2X$. The magnitudes of the six principal transfer integrals supports our derivation of Eq. (4). The main source of the interchain interaction is from t_{I3}, arising between third nearest neighbors, which has relatively little variation over the range of compounds studied, especially for $(TMTSF)_2X$. t_{I2}, the second nearest neighbor coupling, contributes 50% of its value to t_S, but because of its opposite phase actually *reduces* the effective interchain band dispersion near E_F. Surprisingly, t_{I1}, between first nearest neighbor cations, is only around 30% of t_{I2} and t_{I3}, the reason being that I1 has only one close chalcogenide pair contact whereas I2 and I3 have two. Furthermore, the I3 juxtaposition optimizes the pσ-pσ overlap in the interchain direction and is between translationally equivalent neighbors. It is therefore this overlap that one should optimize *vis-a-vis* I1 and I2 in a given structure to increase interchain interaction. Interestingly, this is indeed the case for the superconducting $(BEDT\text{-}TTF)_2ReO_4$ compound[8]. The central role of the I3 interaction has also been established experimentally by Wudl, *et al.*.[9], through x-ray diffraction studies of the electron density distribution in $(TMTSF)_2AsF_6$.

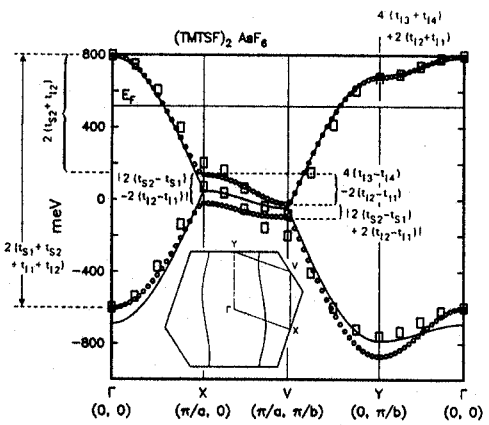

Fig. 3. Band structure of $(TMTSF)_2AsF_6$.

4. High temperature band structure.— Figure 3 shows the band structure and Fermi contour for $(TMTSF)_2AsF_6$ and is representative of all TMTCF compounds. The shape of the Fermi contour is almost indistinguishable between the various Table I-II materials. The position of E_F as measured from the top of the transport band for each compound is given in Tables I-II. The open circles indicate the result obtained from Eqs. (3) and the six $(TMTSF)_2AsF_6$ transfer integrals from Table I, while the solid line arises from substituting t_S and t_I into Eq. (4). The open squares denote the direct diagonalization of Eq. (1) summed to all cation neighbors shown in Fig. 1. The overall agreement with the simple model of Eq. (4) is very good, especially in the vicinity of E_F. Also indicated in Fig. 3 are the dependencies of various band structure features on the six transfer integrals of Eqs. (3).

Since the simple model of Eq. (4) fits so well, we use it to derive the plasma tensor components at E_F by integration of the Boltzman equation[10]. The resulting expressions referred to reciprocal lattice trigonal coordinates are

$$(\hbar^2\omega_p^2)_{a^*a^*} = \frac{8e^2a^2t_S}{V} I_1(t_S/t_I;\ E_F/2t_S) \ , \tag{8a}$$

and

$$(\hbar^2\omega_p^2)_{b^*b^*} = \frac{16e^2b^2t_I^2}{Vt_S} I_2(t_S/t_I;\ E_F/2t_S) \ , \tag{8b}$$

where

$$I_1(A;\ B) = \frac{1}{\pi}\int_0^{\pi}[1-(B-A\cos u)^2]^{1/2}\,du \ , \tag{8c}$$

and

$$I_2(A;\ B) = \frac{2}{\pi}\int_0^{\pi}\frac{\sin^2 u\,du}{[1-(B-A\cos u)^2]^{1/2}} \ . \tag{8d}$$

Here V is the unit cell volume. Note that Eqs. (8) imply $\sigma_a/\sigma_b \propto (t_S/t_I)^2$ unlike that for coherent transport on a closed Fermi contour where σ_a/σ_b is linear in the transfer integral ratio. Thus one cannot differentiate coherent from diffusive transport for open Fermi contours. Equations (8) can now be used to analyze the $(TMTSF)_2PF_6$ optical data of Jacobsen, *et al.*[11]. We find t_S = 321 meV and t_I = 27 meV in excellent agreement with the calculation given the uncertainty in the Drude analysis.

5. Dimensionality in $(TMTCF)_2X$.— These relatively large values of interchain coupling and concomitant small anisotropies for all of the $(TMTSF)_2X$ compounds, now substantiated by both calculation and experiment, impact various ways of looking at the question of quasi-one-dimensionality and attendant fluctuations in these materials. Shultz, *et al.*[12], have developed a Ginzburg-Landau theory for superconducting fluctuations in $(TMTSF)_2X$ which contains a parameter $B = 2\pi^2 t_I^2/\theta$ which is the 3D to 1D fluctuation crossover temperature. Our value of t_I would lead to B = 14000K, well above the vicinity of the superconducting transition implying that mean field theory might be more appropriate. Horowitz, Gutfreund and Weger[13] have derived an expression giving the range of interstack coupling for which Fermi contour nesting can occur and yet mean field conditions still apply:

$$4T_P\left(\frac{\epsilon_0}{T_F}\right) \leq 2t_I \leq 3\epsilon_0\left[\frac{T_P/T_F}{|\alpha|}\right]^{1/2} . \qquad (9)$$

Here T_P is the SDW MI transition temperature, T_F the Fermi temperature as measured from the top of the conduction band, $|\alpha|$ a band filling factor equal to 0.79 for a quarter-empty 1D tight binding band, and $\epsilon_0 = v_F p_F/2 = (\sqrt{2}\pi/8)t_S$, a scaling factor resulting from a density-of-states-like integration over the same tight binding band. The lower limit of Eq. (9) expresses the 1D boundary on $2t_I$ above which mean field theory applies and the upper limit gives the energy below which nesting can be expected. For $(TMTSF)_2AsF_6$, ϵ_0 = 2377K (205 meV), T_F = 3190K (275 meV) and T_P = 12K, yielding 36K and 492K for these two limits, respectively, whereas $2t_I$ = 603K (2×26 meV) suggesting that the selenium compounds are very 2D and nesting should not occur. Since the SDW transition does indeed seem driven by a Fermi instability, the nesting criterion of Horowitz, *et al.*, may be too conservative. On the other hand, for $(TMTTF)_2Br$, in which ϵ_0 = 1545K (133 meV), T_F = 1891K (163 meV) and T_P = 19K, the Eq. (9) upper and lower limits are 62K and 523K, respectively, with $2t_I$ = 232K (2×10 mev). Thus, for the sulfur compounds, as for selenium, the criterion supports a mean field approach to their properties above T_P.

Weger[14] has devised an operational definition of metallic quasi-one-dimensionality based on the mean time a carrier spends in coherent transport along the stack before it is scattered or hops to a neighboring chain. If this time is long compared to the interchain hopping rate, then interchain phase coherence is established, perpendicular quasi-momentum becomes a good quantum number, and we have 2D or 3D transport. On the other hand, if this time is short, phase coherence is inhibited and quasi-1D behavior results. Weger's "golden rule" is contained in the following inequality:

$$E_F > \hbar/\tau_S > t_I . \qquad (10)$$

If $\hbar/\tau_S$ satisfies Eq. (10) at a given temperature and/or pressure, then quasi-1D behavior may be expected, *i.e.*, coherent transport on the stacks, diffusive between them. The uncertainty-principle-like upper limit, $E_F > \hbar/\tau_S$, assures coherent transport on the stacks, otherwise the Fermi contour is washed out. Using the expression $\sigma = \omega_P^2\tau/4\pi$, calculating ω_P from Table I with Eqs. (8), and literature[15] values for conductivity, we obtain $\hbar/\tau_S \approx$ 588 meV for $(TMTSF)_2PF_6$ at 300K. Thus, at room temperature, the chain carrier lifetime energy for the selenium salts is greater than both t_I and E_F. According to Eq. (10) and the experimental conductivity data, quasi-1D conduction begins around 200K with the 1D – 2D crossover at about 55K. In contrast, the sulfur compounds, typified by $(TMTTF)_2Br$[16], with $\hbar/\tau_S \approx$ 840 meV at 300K and 210 meV at the 100K conductivity maximum, appear to have no quasi-1D region, let alone 1D – 2D crossover, whatsoever at ambient pressure. This result is in agreement with Coulon, *et al.*[16]. However, Parkin, *et al.*[17], have shown that the conductivity of the $(TMTTF)_2X$ compounds increases rapidly under applied pressure. Setting $\hbar/\tau_S = E_F$, the threshold conductivity for diffusive-1D coherent crossover for

$(TMTTF)_2Br$ is calculated to be ~1300 $(\Omega cm)^{-1}$ which is reached at room temperature under ~5 kbar of pressure. Likewise, putting $\hbar/\tau_S = t_I$ yields $\sigma \approx 21000$ $(\Omega cm)^{-1}$ as the 1D-2D crossover point. This level of conductivity occurs in $(TMTTF)_2Br$ near T = 100K at P = 26 kbar. Thus, the conclusion of Parkin, *et al.*[17], that the transport behavior of the sulfur salts under pressure approaches that of the selenium compounds at ambient, is supported by the calculations.

Finally, Tables I and II list the 1D dimerization gap relevant to the electron-electron umklapp coupling constant g_3 of g-ology. Our values of the dimerization gap energy do not correlate well with the crystallographic definition of dimerization as used by Emery, *et al.*[18], in their theory relating g_3 to the MI transition temperature and critical pressure for superconductivity in $(TMTCF)_2X$. Since it would appear that cation juxtaposition is at least as important as the magnitude of nearest neighbor interchalcogenide distances in determining g_3 through the dimerization energy gap, the role of electron-electron umklapp scattering in setting T_{MI} and P_c must be re-examined. Such re-examination should also address the rather large dispersion in the dimerization gap when interchain coupling is present and its implication for application of 1D g-ology type theories.

6. Low temperature band structure.— We now consider the effects of low temperature-induced changes in the high temperature translation group of $(TMTCF)_2X$. Two distinct, but possibly related, symmetry breaking mechanisms are known to occur experimentally. A magnetic superlattice of standing SDW's or simple antiferromagnetic (AF) ordering[19] is observed when X is centrosymmetric, and, when X is non-centrosymmetric, the anions order (AO) on a superlattice commensurate with the high temperature crystal structure. For the AF case, no data are currently available on the period of the magnetic superlattice; however, for reasons to be discussed shortly, it is likely to be doubly periodic in all high temperature unit cell directions. For AO, x-ray data indicate doubling of the high temperature unit cell in one, several or all directions at sufficiently low temperature[20]. Here we will only discuss the consequences of commensurate doubling of the direct lattice in the a and/or b directions, or, in terms of reciprocal space translations, the three symmetries Q = (1/2, 0), (1/2, 1/2) and (0, 1/2).

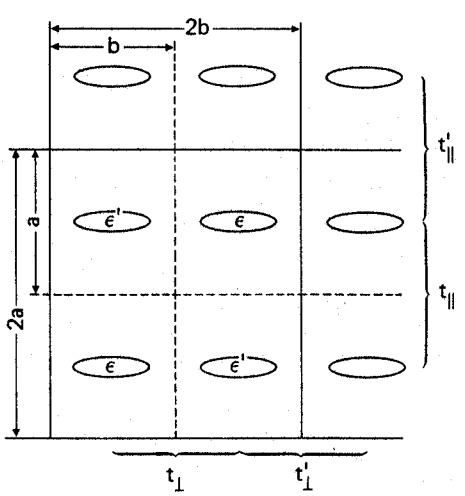

Fig. 4. Idealized schematic of the 2×2 ordered lattice of $(TMTSF)_2X$.

Figure 4 shows an idealized cation arrangement in Q = (1/2, 1/2) symmetry. Each oval contains a single dimer and its net spin. The basic unit of the low temperature model is thus a TMTCF dimer instead of a molecule as at high temperature. We base this *Ansatz* on the belief that the principal perturbation under broken symmetry will be between dimer species rather than within them. The different site energies are given by ϵ, ϵ', arising from AF and/or anion ordering. The interdimer transfer integrals associated with any displacive distortions induced by the anion order are $t_{\|}$, $t_{\|}'$, $t_\perp$ and $t_\perp'$. Under AF ordering, ϵ, ϵ', represent site exchange potentials seen by a passing carrier of given spin[21]. For the AO case, ϵ, ϵ', represent the Madelung potential of the anion lattice. In the examples to follow, we have omitted cation distortion, *i.e.*, we take $t_{\|} = t_{\|}'$ and $t_\perp = t_\perp'$. This simplification of course affects the algebraic dependence of various band structure features, but does not change the qualitative aspects of the induced broken symmetry.

Figure 4 then results in simple fourth order secular equation in the three parameters $\Delta = (\epsilon - \epsilon')/2$, $t_\parallel$ and $t_\perp$. Figure 5 summarizes the solutions to this equation for each of the three symmetries taking $t_\parallel/t_\perp = 10$ in the spirit of Table I, and $\Delta = 2t_\perp$, chosen for illustrative purposes only. Like Fig. 3, the energy axes on Fig. 5 show the dependence of the major band structure features on the model parameters. The k-vector axes are not to scale, but the Brillouin zone insets are.

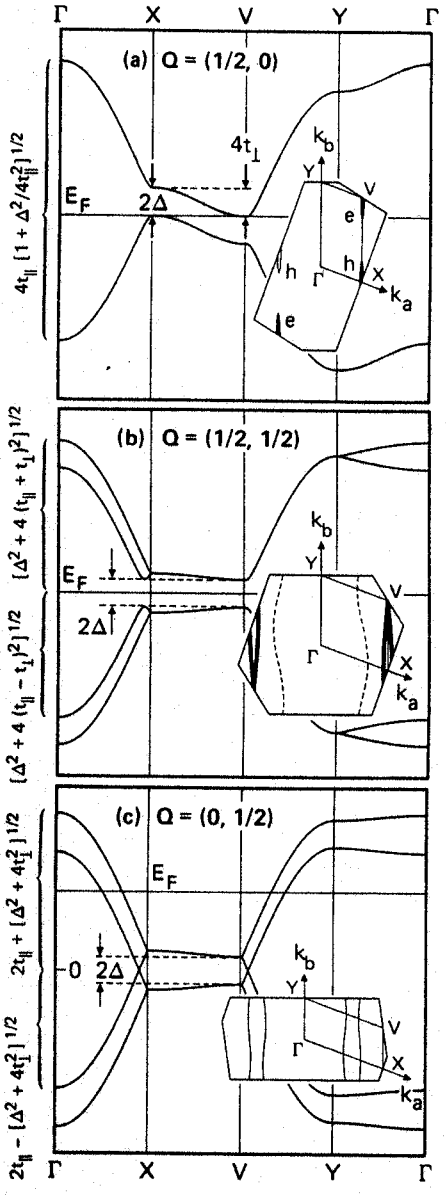

Fig. 5. Model band structures for the three most highly commensurate two-dimensional broken symmetries: (a) Q = (1/2, 0); (b) Q = (1/2, 1/2); (c) Q = (0, 1/2).

Q = (1/2, 0): Depending on the ratio of the Madelung and/or AF exchange parameter Δ and the b-axis bandwidth $4t_\perp$, either a semimetal ($2\Delta < 4t_\perp$) or an indirect gap semiconductor ($2\Delta > 4t_\perp$) can be obtained. Figure 2a explicitly shows $2\Delta = 4t_\perp$, *i.e.*, a zero bandgap semiconductor. The Brillouin zone detail, however, illustrates the more likely semimetallic case ($\Delta/2t_\perp = 2/3$) and the inherent hole-electron pockets. It is known that $(TMTSF)_2NO_3$ undergoes Q = (1/2, 0) AO at 40K, exhibiting a conductivity anomaly[22] and a drop in thermopower[15] at this temperature. Its properties remain metallic down to 12K where a non-magnetic MI transition of unknown (probably AO) origin occurs. These properties between 40-12K are incorporated in our model. Neither superconductivity nor SDW activity appear to be present in $(TMTSF)_2NO_3$[22] consistent with the unfavorable nesting situation and decreased density of states in the semimetallic state.

Q = (1/2, 1/2): Here is a natural model for the AF insulating state found for the centrosymmetric anion compounds. Note that an insulator invariably results with direct gap 2Δ, however weak the exchange interaction. Q = (1/2, 1/2) is the only symmetry of our three that yields an insulator for every finite value of 2Δ. Figure 5b is then the band structure for AF-ordered $(TMTCF)_2X$ (C = Se, X = PF_6, AsF_6, SbF_6, TaF_6; C = S, X = Br, PF_6) and anion ordered $(TMTCF)_2X$ (C = Se, X = ReO_4, (NO_3?); C = S, X = ClO_4, ReO_4), below the MI temperature. The band gap should not be removable by pressure without further symmetry changes. Thus, if pressure could somehow be applied below the MI transition, one should not be able to restore the metallic state. Since the gap is created is created by the removal of a virtual crossing near X, we expect for $2\Delta << 4t_\perp$, $m^* << 1$ with attendant high mobility. The constant energy contours for the electron-hole band extrema form a closed <<trench>> about the X-V direction and are characterized by effective masses $m_\parallel$ and $m_\perp$ reduced from their high temperature values by approximately $\Delta/2t_\parallel$ near X and

$\Delta/2t_\perp$ at V, respectively. Chaikin, *et al.*[23], have estimated $2\Delta \approx 4$ meV for $(TMTSF)_2PF_6$ in its insulating AF state. Using Table I values for $t_\parallel$, $t_\perp$, gives about 1/300 and 1/30 for the two reduction factors. The Q = (1/2, 1/2) model is thus qualitatively consistent with the magnetoresistance[23] and nonlinear[24] data on X = PF_6 below the MI transition.

Q = (0, 1/2): A finite 2Δ does not introduce any gaps near E_F — the number of Fermi contours actually increases from two to four preserving the metallic ground state. X-ray studies show that slowly cooled $(TMTSF)_2ClO_4$ displays this symmetry below 22K due to ClO_4 anion ordering[25] and also remains metallic. An analysis of nesting tendencies in Q = (0, 1/2) symmetry reveals no possibility of creating a commensurate superlattice for a reasonable 2Δ. We believe this feature stabilizes the Q = (0, 1/2) state against SDW formation leaving open the path to superconductivity. Slowly cooled, or <<relaxed>>, $(TMTSF)_2ClO_4$ exhibits a depressed spin-lattice relaxation rate right down to the superconducting transition[26] in agreement with the model, whereas rapidly cooled, or <<quenched>>, samples display an SDW induced MI transition and no superconductivity[27]. Finally, we point out that the discussion of nesting in this symmetry also applies to the recently discovered superconductor $(BEDT\text{-}TTF)_4(ReO_4)_2$[8] where there are two cation stacks per unit cell and the ReO_4 anions alternate in rotational position perpendicular to the stacking axis.

7. Concluding remarks.— We have computed the high temperature single particle electronic structure of $(TMTCF)_2X$ and for C = Se find the average stack bandwidth $4t_S$ = 1.5 eV with mean interchain bandwidth $4t_I$ = 92 meV and resultant anisotropy of 16. For C = S, the values are 0.88 eV, 43 mev and 21, respectively. To the degree that the results can be checked, the agreement with current experiment is excellent. We showed that within the semi-empirical MWH method used in charge transfer salt calculations, use of an extended basis set is crucial to obtain the correct intermolecular overlap behavior. The implications of our findings on dimensionality in $(TMTCF)_2X$ are as follows: (1) the conditions necessary for application of mean field theory to both the selenium and sulfur compounds are satisfied — it is questionable whether a Ginzburg-Landau theory of 1D superconducting fluctuations well above the 3D transition temperature can be justified; (2) in terms of Weger's criteria for quasi-1D *vis-a-vis* 2D coherent or diffusive transport, we find selenium systems to have a 1D-2D crossover at about 60K at 1 bar, while the transport of the sulfur materials is diffusive in all directions at all temperatures above T_{MI} at ambient pressure, exhibiting 1D coherent conductivity and a 1D-2D crossover only at higher pressures; (3) the dimerization gap for C = Se and S does not seem to correlate well with T_{MI} and P_c as required by a quasi-1D g-ology picture involving electron-electron umklapp scattering. For the electronic structure of the $(TMTCF)_2X$ salts at low temperature, we present a set of models based on symmetry breaking of the high temperature structure by antiferromagnetic or anion ordering. In three simple instances of known low temperature anion orderings, we are able to accommodate much, if not all, of the observed behavior in those compounds, and propose a possible magnetic superlattice configuration for the antiferromagnetic compounds.

Acknowledgements.— Throughout the course of the work presented in this paper, we have benefited greatly from interactions with our colleagues in the Organic Solid State Department at the IBM San Jose Research Laboratory. We especially acknowledge many stimulating conversations with S. S. P. Parkin, R. L. Greene, J. C. Scott, J. B. Torrance, E. M. Engler, P. S. Bagus, J. M. Rohr, F. Herman, K. Carneiro and T. C. Clarke.

References

[1] Mol. Cryst. Liq. Cryst. **79** (1981) No. 1. and these proceedings.

[2] P. M. Grant, see these proceedings.

[3] S. P. McGlynn, L. G. Vanquickenborne, M. Kinoshita and D. G. Carroll, *Introduction to Applied Quantum Chemistry*, (Holt, Rinehart and Winston, New York, 1972), p. 97.

[4] E. Clementi and C. Roetti, Atomic Data and Nuclear Data Tables **14** (1974) 177.

[5] P. M. Grant, Phys. Rev. **B16** (1982) 6888. Table I of this paper is superseded by Tables I and II of the present work.

[6] P. M. Grant, to appear in Phys. Rev. B, Rapid Communications. This paper contains a critical assessment of the basis sets used in charge transfer salt MWH band structure calculations.

[7] The crystal structures used in our calculations were taken from:
TMTSF:
PF_6 (300K): N. Thorup, G. Rindorf, H. Soling and K. Bechgaard, Acta Cryst. **B37** (1981) 1236; ReO_4: G. Rindorf, Technical University of Denmark, private communication; ClO_4: K. Bechgaard, K. Carneiro, F. B. Rasmussen, M. Olsen, G. Rindorf, C. S. Jacobsen, H. J. Pedersen and J. C. Scott, J. Am. Chem. Soc. **103** (1981) 2440; AsF_6: F. Wudl, J. Am. Chem. Soc. **103** (1981) 7065. and private communication; FSO_3: J. M. Williams, M. A. Beno, E. H. Appelman, J. M. Capriotti, F. Wudl, E. Aharon-Shalom and D. Nalewajek, Mol. Cryst. Liq. Cryst. **79** (1982) 319; PF_6 (4K):H. E. King and S. J. La Placa, Bull. Am. Phys. Soc. **26** (1981) 214. NO_3: H. Soling, G. Rindorf and N. Thorup, submitted to Crystal Structure Communications; H_2F_3: J. M. Williams, private communication.
TMTTF:
Br: J. L. Galigné, B. Liautard, S. Peytavin, G. Brun, J. M. Fabre, E. Torreilles and L. Giral, Acta. Cryst. **B34** (1978) 620; BF_4: J. L. Galigné, B. Liautard, S. Peytavin, G. Brun, M. Maurin, J. M. Fabre, E. Torreilles and L. Giral, Acta. Cryst. **B35** (1979) 1129; SCN: J. L. Galigné, B. Liautard, S. Peytavin, G. Brun, M. Maurin, J. M. Fabre, E. Torreilles and L. Giral, Acta. Cryst. **B35** (1979) 2609; ReO_4: S. S. P. Parkin and J. J. Mayerle, private communication.

[8] S. S. P. Parkin, E. M. Engler, R. R. Schumaker, R. Lagier, V. Y. Lee, J. C. Scott and R. L. Greene, to be published in Phys. Rev. Letters.

[9] F. Wudl, D. Nalewajek, J. M. Troup and M. W. Extine, to be published in Science.

[10] A similar calculation has been performed by J. F. Kwak, Phys. Rev. **B26** (1982) 4789.

[11] C. S. Jacobsen, D. B. Tanner and K. Bechgaard, Phys. Rev. Letters **46** (1981) 1142; C. S. Jacobsen, D. B. Tanner and K. Bechgaard, Mol. Cryst. Liq. Cryst. **79** (1982) 25.

[12] H. J. Schulz, D. Jerome, A. Mazaud, M. Ribault and K. Bechgaard, J. Physique **42** (1981) 991.

[13] B. Horowitz, H. Gutfreund and M. Weger, Phys. Rev. **B12** (1975) 3174.

[14] M. Weger, Bull. Europ. Phys. Soc. **9** (1978) 7.

[15] K. Bechgaard, C. S. Jacobsen, K. Mortensen, H. J. Pedersen and N. Thorup, Solid State Commun. **33** (1980) 1119.

[16] C. Coulon, P. Delhaes, S. Flandrois, R. Lagnier, E. Bonjour and J. M. Fabre, J. Physique **43** (1982) 1059.

[17] S. S. P. Parkin, F. Creuzet, D. Jerome, J. M. Fabre and K. Bechgaard, to be published in J. Physique.

[18] V. J. Emery, R. Bruinsma and S. Barisic, Phys. Rev. Letters **48** (1982) 1039.

[19] K. Mortensen, Y. Tomkiewicz and K. Bechgaard, Phys. Rev. **B25** (1982) 3319.

[20] J. P. Pouget, R. Moret, R. Comes, K. Bechgaard, J. M. Fabre and L. Giral, Mol. Cryst. Liq. Cryst. **79** (1982) 129; S. S. P. Parkin, D. Jerome and K. Bechgaard, Mol. Cryst. Liq. Cryst. **79** (1982) 213.

[21] J. C. Slater, Phys. Rev. **82** (1951) 538.

[22] S. S. P. Parkin, F. Creuzet, D. Jerome and K. Bechgaard, to be published in J. Physique.

[23] P. M. Chaikin, P. Haen, E. M. Engler and R. L. Greene, Phys. Rev. **B24** (1981) 7155.

[24] P. M. Chaikin, G. Gruner, E. M. Engler and R. L. Greene, Phys. Rev. Letters **45** (1980) 1874; E. N. Conwell and N. C. Banik, Mol. Cryst. Liq. Cryst. **79** (1982) 95.

[25] J. P. Pouget, G. Shirane, K. Bechgaard and J. M. Fabre, to be published in Phys. Rev. Letters.

[26] T. Takahashi, D. Jerome and K. Bechgaard, J. Physique-Lett. 43 (1982) 573.

[27] S. Tomic, D. Jerome, P. Monod and K. Bechgaard, see these proceedings.